The Jahn-Teller vibronic reduction factors in icosahedral $G \otimes (g \oplus h)$ systems

2002 J. Phys.: Condens. Matter 14 4679

(http://iopscience.iop.org/0953-8984/14/18/305)

INSTITUTE OF PHYSICS PUBLISHING JOURNAL OF PHYSICS: CONDENSED MATTER

J. Phys.: Condens. Matter **14** (2002) 4679–4697 PII: S0953-8984(02)31922-2

The Jahn–Teller vibronic reduction factors in icosahedral $G \otimes (g \oplus h)$ systems

M Abou-Ghantous[1], P B Oliete[2,3], C A Bates[2], J L Dunn[2], V Z Polinger[2], R Huang[2,4] and S P Rough[2,5]

[1] Department of Physics, CAMS, American University of Beirut, Beirut, Lebanon
[2] School of Physics and Astronomy, University of Nottingham, University Park, Nottingham NG7 2RD, UK
[3] Instituto de Ciencia de Materiales de Aragon, Departamento de Fisica de la Materia Condensada, Facultad de Ciencias, Pza S. Francisco s/n, Zaragoza 50009, Spain

E-mail: Colin.Bates@nottingham.ac.uk and Janette.Dunn@nottingham.ac.uk

Received 14 December 2001, in final form 21 February 2002
Published 26 April 2002
Online at stacks.iop.org/JPhysCM/14/4679

Abstract

Analytical expressions for the vibronic states and energy spectrum of the icosahedral $G \otimes (g \oplus h)$ Jahn–Teller system are derived. From these states, expressions for first- and second-order vibronic reduction factors are determined as a function of the strengths of the coupling of the G orbital to the g and h modes of vibration. The possibility of the vibronic ground state being a singlet A state, rather than the G state that would be expected in the absence of vibronic coupling, is explored. The reduction factors obtained provide a convenient basis for the modelling of spectra involving some of the excited states of the fullerene molecule C_{60} and related ions.

1. Introduction

Electron–phonon interactions, via the Jahn–Teller (JT) effect, can have a strong influence on the electronic states of molecules and ions. However, JT effects involving an orbital quadruplet G have received little attention in the literature, despite the fact that the G quadruplet is an excited state of the $C_{60}^{\pm}$ molecules and probably also the ground state of both C_{80}^{+} and the cage isomer of C_{20}^{+} [1], and of Si_{13}^{+} clusters [2]. Furthermore, it has become clear in recent years that the electron–phonon interaction plays an important role in understanding many of the properties of these and other fullerene molecules.

There are five irreducible representations (irreps) in the icosahedral group I_h, namely a singlet A, triplets T_1 and T_2, a quadruplet G and a quintet H [3–6]. A study of the products of the irreps shows that six JT couplings need to be considered in I_h symmetry. Those JT effects

[4] Present address: MR Group, Insitute of Medicine, Research Centre Julich, 52425 Julich, Germany
[5] Present address: J P Morgan, 1 Angel Row, London EC2R 7AE, UK.

involving only single modes are written in the form $\Gamma \otimes \Lambda$, where Γ is the electronic state and Λ is the vibrational state. The possible JT effects are thus $T_1 \otimes h$, $T_2 \otimes h$, $G \otimes g$, $G \otimes h$, $H \otimes g$ and $H \otimes h$. However, coupling to more than a mode of a single symmetry is possible. In particular, the G orbital can couple to both g and h vibrations in a $G \otimes (g \oplus h)$ JT effect. $G \otimes g$ and $G \otimes h$ can be considered as subsystems of the more general $G \otimes (g \oplus h)$ case.

It appears that the first example of G states studied in any detail involved icosahedral structures of boron [7–9]. In 1978, Khlopin *et al* [10] analysed a number of the simpler icosahedral systems from a theoretical point of view including the $G \otimes h$ subsystem. Other theoretical work has since been undertaken by Pooler [6] for the regime in which the g and h modes were equally coupled, and by Ceulemans and Fowler [1] who obtained highly significant results from an analysis of the adiabatic potential energy surface (APES) for the $G \otimes (g \oplus h)$ problem. Subsequently, Cullerne and O'Brien [11] discussed the phases and topography of the lowest APES for the same system. These issues and their context are described in the book of Chancey and O'Brien [12].

An important application of JT theory relates to effective Hamiltonians that can be constructed to model the effects of perturbations such as spin–orbit coupling, strain and magnetic fields. RFs are introduced as parameters in an effective Hamiltonian so that an electronic perturbation V can be described in terms of a purely electronic Hamiltonian. The idea of RFs in JT systems was first proposed by Ham in 1965 [13] who showed that a dynamic JT effect can cause large changes in the magnitudes of some matrix elements of electronic operators. First-order RFs arise when V occurs once in a perturbation calculation; second-order RFs arise when V occurs twice. It is well known that second-order RFs can become particularly important in some cases of strong coupling. They introduce additional terms in the resultant effective Hamiltonian and, because the effect of the first-order terms can be significantly reduced, the contributions of the second-order RFs can then dominate. Thus both first- and second-order RFs need to be calculated.

RFs implicitly incorporate the effect of the phonons into the electronic terms which increases the electron effective mass. This in turn contributes significantly to reductions in the energy gaps in the electron energy spectrum. This spectrum is the main architect for the modelling of spectroscopic data. Because the RFs contain the effects of the vibronic couplings, essential physics can be bypassed if the RFs are simply regarded as free parameters adjusted to fit experimental data rather than as important real physical parameters in their own right. It appears that the only calculations of RFs for the orbital quadruplet are those given by [14] which are for the limit of strong vibronic coupling.

The object of this paper is to analyse the $G \otimes (g \oplus h)$ JT system and calculate the RFs for this system and its subsystems covering all ranges of coupling strengths to the two modes. The methodology to be used here follows that described by the authors for the analytical calculation of the first- and second-order RFs for the $T \otimes h$ [15] and $H \otimes (g \oplus h)$ JT systems [16], although the nature of the high symmetries involved means that application to this system is far from trivial. It is sufficient for our purposes here to limit the discussion to linear JT interactions (in which the normal-mode coordinates enter the interaction in linear fashion) since these are capable of illustrating the general features of vibronic couplings considered in this paper.

2. The theoretical model

A good starting point for the analysis of JT systems is to analyse the ground APES. In some other cases, there is a trough of minimum-energy points, but in most cases the surface contains a number of distinct wells (minima). In very strong coupling, a 'static' picture is appropriate in which the motion consists of vibrations in these wells. However, when the barriers between

the wells are not infinite, a dynamic picture holds and tunnelling between equivalent wells will occur. Consequently, the prevailing degeneracy on the vibronic states is completely or partially lifted and the resulting vibronic states, transforming with the required symmetry, are linear combinations of the states localized in the wells.

One analytical method in which wells can be generated is the shift transformation (ST) method [17] with the positions of the wells fixed using a method developed by Öpik and Pryce [18]. Projection operator techniques can then be used to obtain symmetry-adapted combinations of the well states that allow for tunnelling between the wells. These procedures have already been used successfully to determine the symmetry-adapted ground and tunnelling states for the icosahedral $T_1 \otimes h$ [19] and $H \otimes (h \oplus g)$ [20] JT systems. Symmetry-adapted vibronic states for the $G \otimes (g \oplus h)$ JT system will now be determined. This procedure is similar in some respects to that used by Ceulemans and Fowler [1] who concentrate on issues concerning the curvature of the APES. The energies associated with the vibronic states will then be calculated and the tunnelling splitting associated with each type of minimum determined. Such a calculation is important because the theoretical results can then be compared directly with experimental transition energy data.

Before proceeding, we comment that only one vibration of each symmetry type will be considered. In real systems, a number of modes of the same symmetry would be coupled. Their inclusion would lead naturally towards the development of a more realistic multimode model. However, on the basis of previous multimode work [21, 22], it can be shown that the extremal properties of this surface are independent of the number of fourfold- and fivefold-degenerate modes included. Much of the behaviour of the system can be obtained from consideration of a single effective mode only. Furthermore, the experimental data available are not sufficiently sophisticated to be of use in distinguishing multimode effects at the present time.

It is now necessary to consider the model Hamiltonian for the icosahedral $G \otimes (g \oplus h)$ JT system. In order that uniformity exists between this and previously published work, particular conventions will be adopted. In order to conform with the work by Ceulemans and Fowler [1], we follow Boyle and Parker [23] and define a twofold axis of quantization together with a coordinate system in which the irreducible representation has canonical components γ labelled a, x, y, z for G states and θ, ε, 4, 5, 6 for H states. Adopting these conventions and using the tables of Fowler and Ceulemans [24] for the Clebsch–Gordan (CG) coefficients, the required model Hamiltonian is

$$\mathcal{H} = \sum_{\Gamma\gamma}\left(\frac{P_{\Gamma\gamma}^2}{2\mu} + \frac{1}{2}\mu\omega_\Gamma^2\right)Q_{\Gamma\gamma}^2 + \mathcal{H}_{int} \tag{1}$$

where $Q_{\Gamma\gamma}$ and $P_{\Gamma\gamma}$ denote the JT-active displacement coordinates and their conjugate momenta respectively, with γ running over the components of the mode Γ (=G and H), μ is the mass of each of the nuclei at the corners of the icosahedron and ω_Γ is the mode frequency. Also $\mathcal{H}_{int}$ is the linear vibronic interaction Hamiltonian given in matrix form with respect to the basis defined above by

$$\mathcal{H}_{int} = \frac{V_g}{2\sqrt{3}}\begin{pmatrix} 3Q_a & -Q_x & -Q_y & -Q_z \\ -Q_x & -Q_a & -\sqrt{5}Q_z & -\sqrt{5}Q_y \\ -Q_y & -\sqrt{5}Q_z & -Q_a & -\sqrt{5}Q_x \\ -Q_z & -\sqrt{5}Q_y & -\sqrt{5}Q_x & -Q_a \end{pmatrix} + \frac{V_h}{\sqrt{15}}\begin{pmatrix} 0 & \sqrt{5}Q_4 & \sqrt{5}Q_5 & \sqrt{5}Q_6 \\ \sqrt{5}Q_4 & -\sqrt{2}(Q_\theta - \sqrt{3}Q_\varepsilon) & -Q_6 & -Q_5 \\ \sqrt{5}Q_5 & -Q_6 & -\sqrt{2}(Q_\theta + \sqrt{3}Q_\varepsilon) & -Q_4 \\ \sqrt{5}Q_6 & -Q_5 & -Q_4 & 2\sqrt{2}Q_\theta \end{pmatrix} \tag{2}$$

where V_g and V_h are the linear coupling constants associated with G and H modes respectively.

Following the transformation method developed in [17], a unitary transformation of the form

$$U = \exp\left(\mathrm{i}\sum_{\Gamma\gamma}\alpha_{\Gamma\gamma}P_{\Gamma\gamma}\right) \tag{3}$$

is introduced and applied to the Hamiltonian $\mathcal{H}$. This displaces the origin of the coordinate $Q_{\Gamma\gamma}$ to $(Q_{\Gamma\gamma} - \alpha_{\Gamma\gamma}\hbar)$ and transforms the Hamiltonian $\mathcal{H}$ such that

$$\tilde{\mathcal{H}} = U^{-1}\mathcal{H}U = \tilde{\mathcal{H}}_1 + \tilde{\mathcal{H}}_2 \tag{4}$$

where $\tilde{\mathcal{H}}_1$ does not contain any $P_{\Gamma\gamma}$s or $Q_{\Gamma\gamma}$s, and hence no phonon operators. $\tilde{\mathcal{H}}_2$ contains all the remaining terms. It follows that $\tilde{\mathcal{H}}_1$ is a good Hamiltonian for determining the ground states of the system in strong coupling.

The energy minimization procedure of Öpik and Pryce [18] is now applied to $\tilde{\mathcal{H}}_1$. It is found that the lowest-energy points can be either tetrahedral (T) or trigonal (D_3) minima, depending upon the values of the coupling constants. The electronic eigenstates and JT stabilization energies are exactly equivalent to those obtained by Ceulemans and Fowler [1] and given in their table 3. The minima in T correspond to the $G \otimes g$ subsystem because no coupling to the h modes occurs in this case. They form what has been called the α-orbit [1]. In terms of the coupling constant defined in this paper, the energy of the T points is

$$E_{JT}^{(g)} = -\frac{3}{8}\frac{V_g^2}{\hbar\mu\omega_g^2}. \tag{5}$$

The T wells are minima when the g mode is dominant such that $E_{JT}^{(g)} < E_{JT}^{(h)} < 0$, where

$$E_{JT}^{(h)} = -\frac{3}{10}\frac{V_h^2}{\hbar\mu\omega_h^2}. \tag{6}$$

The D_3 points are saddle points in this case.

The D_3 points involve both sets of modes in the $G \otimes (g \oplus h)$ system, and form the so-called β-orbit [1]. The energy of these points is

$$\tfrac{2}{27}E_{JT}^{(g)} + \tfrac{25}{27}E_{JT}^{(h)}. \tag{7}$$

These are minima (and the T points are saddle points) when the h mode is dominant ($E_{JT}^{(h)} < E_{JT}^{(g)} < 0$). Clearly, in the case where the JT stabilization energies $E_{JT}^{(g)}$ and $E_{JT}^{(h)}$ are equal, neither mode is more stable; this situation corresponds to the degenerate coupling case when the JT distortion space becomes an equipotential minimal energy trough [25–27]. In addition to the minima mentioned above, two other sets of extrema occur having trigonal and dihedral symmetry are present. As they always correspond to saddle points, they do not feature in calculations leading to the derivation of the vibronic tunnelling states or the energies associated with these states.

3. Analytical form of the vibronic states

3.1. Basis states

As outlined above, the required vibronic ground states are derived from the eigenstates of $\mathcal{H}$ localized in either the tetrahedral or trigonal wells as appropriate. In general, the ground vibronic state in well k is written in the form $|\psi_k; 0\rangle$, where ψ_k corresponds to the ground electronic state in well k, with '0' indicating that the phonons are all in their ground state.

These states may be transformed back to the original space by operating on them with the unitary operator $U = U_k$ appropriate to well k, after substitution of the suitable values of $\alpha_{\Gamma\gamma}$. Hence, the untransformed well state becomes

$$|\psi'_k; 0\rangle = U_k|\psi_k; 0\rangle \tag{8}$$

which is automatically vibronic as a consequence of the unitary transformation which contains phonon operators. It is now necessary to take symmetrized combinations of these well states to obtain states appropriate for finite coupling. Such a linear combination of states may be constructed using projection operator techniques. The basic theory of projection operators is described in detail in [28].

3.2. Vibronic ground states corresponding to the tetrahedral wells

Following the procedures outlined above, the symmetry-adapted vibronic ground states corresponding to the tetrahedral wells (and labelled by the superscript T) have symmetries A and G. They may be written as specific combinations of the orbital states ψ_k in the wells. The wells will be labelled A–E, and the ψ_k for these wells are given in column 1 of table 3 in [1] The symmetry-adapted states have the form

$$\begin{aligned}
|A_a^T\rangle &= \frac{1}{\sqrt{5}} N_A^T[|A';0\rangle + |B';0\rangle + |C';0\rangle + |D';0\rangle + |E';0\rangle] \\
|G_a^T\rangle &= \frac{1}{2\sqrt{3}} N_G^T[4|A';0\rangle - |B';0\rangle - |C';0\rangle - |D';0\rangle - |E';0\rangle] \\
|G_x^T\rangle &= \tfrac{1}{2} N_G^T[-|B';0\rangle - |C';0\rangle + |D';0\rangle + |E';0\rangle] \\
|G_y^T\rangle &= \tfrac{1}{2} N_G^T[-|B';0\rangle + |C';0\rangle - |D';0\rangle + |E';0\rangle] \\
|G_z^T\rangle &= \tfrac{1}{2} N_G^T[-|B';0\rangle + |C';0\rangle + |D';0\rangle - |E';0\rangle]
\end{aligned} \tag{9}$$

where the N_i^T are normalization factors for vibronic states of symmetries A and G given by

$$\begin{aligned}
N_A^T &= (1 + 4S_{12}^T)^{-1/2} \\
N_G^T &= (1 - S_{12}^T)^{-1/2}
\end{aligned} \tag{10}$$

respectively. S_{12}^T is the overlap between any two of the vibronic ground states in different wells given by

$$S_{12}^T = -\tfrac{1}{4} \exp(-\tfrac{15}{16} k_g^2) \tag{11}$$

where

$$k_g = -V_g/(2\mu\hbar\omega_g^3)^{1/2}. \tag{12}$$

3.3. Vibronic ground states corresponding to the trigonal wells

Following a similar procedure, the symmetry-adapted vibronic ground states have symmetries A, G and H. They may be written as specific combinations of the orbital states ψ_k in the trigonal wells. The wells are labelled a–j, and the ψ_k are given in column 2 of table 3 in [1].

The required symmetry-adapted vibronic ground states for the trigonal wells are

$$
\begin{aligned}
|A_a^{D_3}\rangle &= \frac{1}{\sqrt{10}} N_A^{D_3}[|a';0\rangle + |b';0\rangle + |c';0\rangle + |d';0\rangle + |e';0\rangle + |f';0\rangle \\
&\qquad + |g';0\rangle + |h';0\rangle + |i';0\rangle + |j';0\rangle] \\
|G_a^{D_3}\rangle &= \frac{1}{\sqrt{60}} N_G^{D_3}[-2(|a';0\rangle + |b';0\rangle + |c';0\rangle + |d';0\rangle + |e';0\rangle + |f';0\rangle) \\
&\qquad + 3(|g';0\rangle + |h';0\rangle + |i';0\rangle + |j';0\rangle)] \\
|G_x^{D_3}\rangle &= \frac{1}{\sqrt{12}} N_G^{D_3}[2(|a';0\rangle - |b';0\rangle) + (-|g';0\rangle - |h';0\rangle + |i';0\rangle + |j';0\rangle)] \\
|G_y^{D_3}\rangle &= \frac{1}{\sqrt{12}} N_G^{D_3}[2(|c';0\rangle - |d';0\rangle) + (-|g';0\rangle + |h';0\rangle - |i';0\rangle + |j';0\rangle)] \\
|G_z^{D_3}\rangle &= \frac{1}{\sqrt{12}} N_G^{D_3}[2(|e';0\rangle - |f';0\rangle) + (-|g';0\rangle + |h';0\rangle + |i';0\rangle - |j';0\rangle)] \\
|H_\theta^{D_3}\rangle &= \frac{1}{\sqrt{12}} N_H^{D_3}[-|a';0\rangle - |b';0\rangle - |c';0\rangle - |d';0\rangle + 2|e';0\rangle + 2|f';0\rangle] \\
|H_\varepsilon^{D_3}\rangle &= \tfrac{1}{2} N_H^{D_3}[|a';0\rangle + |b';0\rangle - |c';0\rangle - |d';0\rangle] \\
|H_4^{D_3}\rangle &= \frac{1}{\sqrt{6}} N_H^{D_3}[(-|a';0\rangle + |b';0\rangle) + (-|g';0\rangle - |h';0\rangle + |i';0\rangle + |j';0\rangle)] \\
|H_5^{D_3}\rangle &= \frac{1}{\sqrt{6}} N_H^{D_3}[(-|c';0\rangle + |d';0\rangle) + (-|g';0\rangle + |h';0\rangle - |i';0\rangle + |j';0\rangle)] \\
|H_6^{D_3}\rangle &= \frac{1}{\sqrt{6}} N_H^{D_3}[(-|e';0\rangle + |f';0\rangle) + (-|g';0\rangle + |h';0\rangle + |i';0\rangle - |j';0\rangle)].
\end{aligned}
\tag{13}
$$

The normalizing factors $N_i^{D_3}$ are given by

$$
\begin{aligned}
N_A^{D_3} &= (1 + 3S_{12}^{D_3} + 6S_{13}^{D_3})^{-1/2} \\
N_G^{D_3} &= (1 - 2S_{12}^{D_3} + S_{13}^{D_3})^{-1/2} \\
N_H^{D_3} &= (1 + S_{12}^{D_3} - 2S_{13}^{D_3})^{-1/2}
\end{aligned}
\tag{14}
$$

where $S_{12}^{D_3}$ and $S_{13}^{D_3}$ denote two different overlaps between trigonal wells given by

$$
\begin{aligned}
S_{12}^{D_3} &= -\tfrac{2}{3} t^2 T \\
S_{13}^{D_3} &= \tfrac{1}{6} t T^2
\end{aligned}
\tag{15}
$$

where

$$
\begin{aligned}
t &= \exp(-\tfrac{5}{108} k_g^2) \\
T &= \exp(-\tfrac{10}{27} k_h^2)
\end{aligned}
\tag{16}
$$

with

$$
k_h = -V_h/(2\mu\hbar\omega_h^3)^{1/2}. \tag{17}
$$

For coupling to the h mode only, $S_{12}^{D_3}$ represents the overlap between nearest-neighbour wells and $S_{13}^{D_3}$ that between next-nearest neighbours. For coupling to the g mode only, this situation is reversed.

4. Energies of the symmetry-adapted states

The degeneracy of the vibronic basis states is partially lifted by taking the symmetry-adapted combinations of states. The symmetry-adapted states derived in section 3 contain Γ ground vibronic states and $(\Lambda$–$\Gamma)$ tunnelling levels, where Λ is the number of wells. The energies corresponding to these states have been obtained by evaluating all the matrix elements of the full Hamiltonian $\mathcal{H}$ between all the untransformed vibronic well states in equations (9) and (13).

4.1. Energies of the vibronic states associated with the tetrahedral wells

On evaluation of all the relevant matrix elements, we find that only two different types of matrix element occur. Within one well, the matrix element has energy E_{11} given by

$$E_{11}^T = (2 - \tfrac{3}{4}k_g^2)\hbar\omega_g + \tfrac{5}{2}\hbar\omega_h \tag{18}$$

while the matrix element between any next-nearest-neighbour wells is

$$E_{12}^T = S_{12}^T[(2 - \tfrac{27}{16}k_g^2)\hbar\omega_g + \tfrac{5}{2}\hbar\omega_h]. \tag{19}$$

The energies of the G and A vibronic states are then given by

$$\begin{aligned} E_A^T &= \frac{E_{11}^T + 4E_{12}^T}{1 + 4S_{12}^T} \\ E_G^T &= \frac{E_{11}^T - E_{12}^T}{1 - S_{12}^T}. \end{aligned} \tag{20}$$

Thus the tunnelling splitting $\delta = E_A^T - E_G^T$ between the A and G states is given by

$$\delta = \frac{5(E_{12}^T - S_{12}^T E_{11}^T)}{1 + 3S_{12}^T - 4(S_{12}^T)^2}. \tag{21}$$

δ is positive for all values of the coupling strength k_g (and is independent of the h-mode coupling k_h). In figure 1, δ is plotted as a function of the coupling strength k_g. It can be seen that in the weak-coupling limit, when the vibrational part of the Hamiltonian dominates the JT interaction, the A state is $\hbar\omega_g$ above the G ground state and corresponds to a state with one-phonon excitation. In the strong-coupling limit, δ approaches zero exponentially as expected through the dominant term involving the overlap S. This result is consistent with that obtained by Cullerne and O'Brien [11] when allowance is made for the differences in signs of the overlap and the energies of the two oscillators in neighbouring wells.

4.2. Energies of the vibronic states associated with the trigonal wells

In a similar way, the energies of the vibronic states associated with the trigonal wells may be determined. In this case there are two distinct matrix elements of $\mathcal{H}$ between well states to determine, which will be denoted by E_{12} and E_{13} (analogous to S_{12} and S_{13}), as well as the energy E_{11} of $\mathcal{H}$ within one well. We find that

$$\begin{aligned} E_{11}^{D_3} &= 2\hbar\omega_g(1 - \tfrac{1}{36}k_g^2) + \tfrac{5}{2}\hbar\omega_h(1 - \tfrac{2}{9}k_h^2) \\ E_{12}^{D_3} &= S_{12}^{D_3}[\hbar\omega_g(2 - \tfrac{4}{27}k_g^2) + \tfrac{5}{2}\hbar\omega_h(1 - \tfrac{10}{27}k_h^2)] \\ E_{13}^{D_3} &= S_{13}^{D_3}[\hbar\omega_g(2 - \tfrac{11}{108}k_g^2) + \tfrac{5}{2}\hbar\omega_h(1 - \tfrac{14}{27}k_h^2)]. \end{aligned} \tag{22}$$

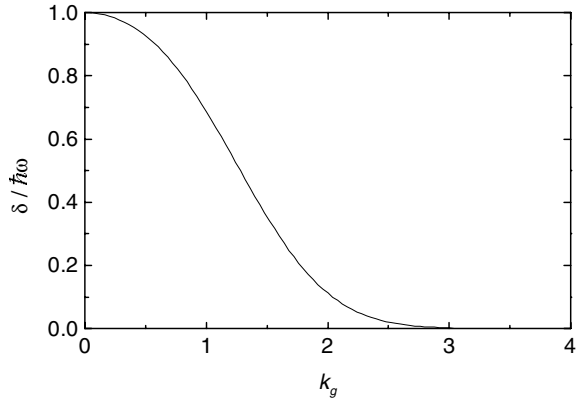

Figure 1. The tunnelling splitting δ as a function of the coupling constant k_g associated with vibronic states of T symmetry.

The energies of the A, G and H tunnelling states are then given by

$$\begin{aligned} E_A^{D_3} &= \frac{E_{11}^{D_3} + 3E_{12}^{D_3} + 6E_{13}^{D_3}}{1 + 3S_{12}^{D_3} + 6S_{13}^{D_3}} \\ E_G^{D_3} &= \frac{E_{11}^{D_3} - 2E_{12}^{D_3} + E_{13}^{D_3}}{1 - 2S_{12}^{D_3} + S_{13}^{D_3}} \\ E_H^{D_3} &= \frac{E_{11}^{D_3} + E_{12}^{D_3} - 2E_{13}^{D_3}}{1 + S_{12}^{D_3} - 2S_{13}^{D_3}}. \end{aligned} \tag{23}$$

The tunnelling splittings $\delta_1 = E_A^{D_3} - E_G^{D_3}$ and $\delta_2 = E_H^{D_3} - E_G^{D_3}$ are functions of both k_g and k_h. Before proceeding, we should note that these results are only valid when the D_3 points are absolute minima. From equations (5) to (7), we can see that in the linear coupling regime considered in this paper, this occurs for $k_h^2 > 5k_g^2/4$. However, it is possible that higher-order contributions to the vibronic coupling, such as bilinear terms, could both turn the D_3 points into minima and lower their energy below that of the T points in certain cases. Indeed, an equivalent effect has been shown to be possible in the cubic $T \otimes (e \oplus t_2)$ JT system [30]. We have therefore plotted δ_1 and δ_2 in figures 2 and 3 respectively as functions of both k_g and k_h for both the region $k_h^2 > 5k_g^2/4$ where the current results are valid and outside this region. We have taken $\omega_g = \omega_h = \omega$ as far as the plots are concerned. It can be seen that both δ_1 and δ_2 tend to zero in the strong-coupling limit, as for the tunnelling splitting with T-symmetry wells. δ_2 varies smoothly from $\hbar\omega$ in weak coupling to 0 in strong coupling (to either mode). However, the mathematical behaviour of δ_1 is somewhat more surprising in both weak and strong coupling. For illustrative purposes, we give a 2D plot of the tunnelling splitting for $k_g = 0$ (curve a) and $k_h = 0$ (curve b) in figure 4, although it must be remembered that the linear coupling results are not actually valid for the coupling represented by curve b.

The limit attained in weak coupling depends upon whether k_g or k_h tends to zero first. As figure 4 shows, the limit is $\hbar\omega$ if k_h is set to zero, whereas if k_g is set to zero, the limit is $2\hbar\omega$. The limit attained when approaching the origin along the boundary of the region of validity is $\hbar\omega$. This is due to the dominance of the contributions from terms in k_g. A similar dual-limit at the origin was found previously for the $H \otimes (g \oplus h)$ JT system [20]. The weak-coupling

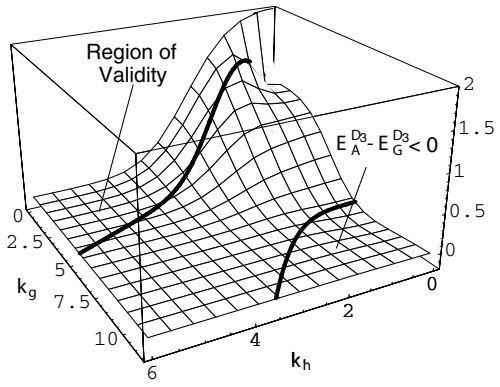

Figure 2. The tunnelling splitting $\delta_1 = E_A^{D_3} - E_G^{D_3}$ as a function of both k_g and k_h for states derived using the D_3 points. Note that the origin ($k_g = k_h = 0$) is at the back corner (in order to show the weak-coupling behaviour) but the axis labels are on the front edges (to be visible). The marked 'region of validity' is that for which the D_3 points are minimum-energy wells in linear coupling.

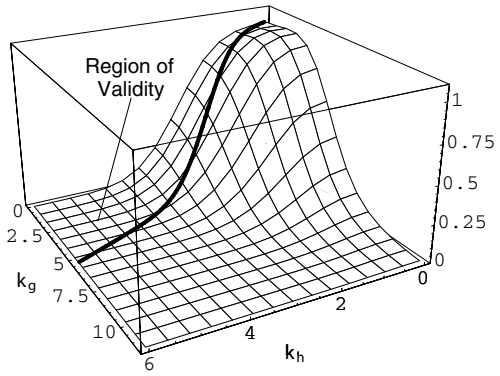

Figure 3. As figure 2 but for the tunnelling splitting $\delta_2 = E_H^{D_3} - E_G^{D_3}$ for states derived using the D_3 points.

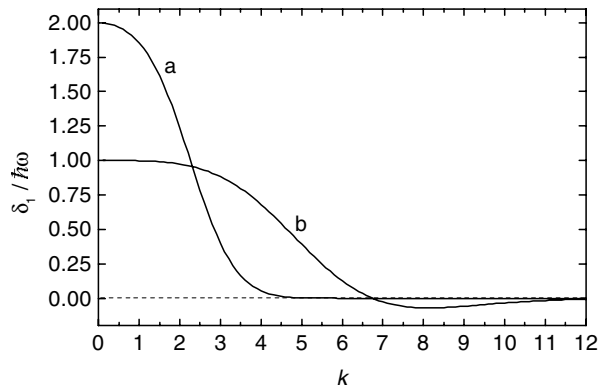

Figure 4. The tunnelling splitting δ_1 as a function of $k = k_h$ for $k_g = 0$ (curve a) and $k = k_g$ for $k_h = 0$ (curve b), both for wells of D_3 symmetry.

limits of both δ_1 and δ_2 can be explained by an examination of the products

$$\begin{aligned} G \otimes G &= A \oplus T_1 \oplus T_2 \oplus G \oplus H \\ G \otimes H &= T_1 \oplus T_2 \oplus G \oplus 2H \\ H \otimes H &= A \oplus T_1 \oplus T_2 \oplus 2G \oplus 2H \end{aligned} \tag{24}$$

and by considering which phonons couple to the electronic orbital states to produce the first tunnelling states. If an electronic state of G symmetry couples to a single phonon of h symmetry, a H electronic state can be formed from the $G \otimes h$ product shown in equation (24). Since only one phonon is involved in this JT interaction, this state will tend to the relative energy $\hbar\omega_h$ in the weak-coupling limit. Likewise, an A vibronic state can also be formed from a G electronic state with a single g-type phonon. In contrast, an A vibronic state cannot be formed from a single h-type phonon. Instead, two h-type phonons must couple together with the electronic G orbital state, as described by a $G \otimes h \otimes h$ JT interaction. Since two phonons have taken part in this interaction, the relative energy of this A vibronic state in the weak-coupling limit is $2\hbar\omega_h$, as is observed.

The strong-coupling behaviour of δ_1 is even more surprising than its weak-coupling behaviour. As figures 3 and 4 show, there is a region of coupling to the g and h modes for which the tunnelling splitting is negative. Although this lies outside the region of validity for the linear coupling results, it does suggest that the possibility of having a singlet ground state cannot be ruled out for some value of vibronic coupling constants when higher-order terms are included. Such a situation is highly significant, because it means that the presence of vibronic coupling can alter the ground state from the quadruplet expected in the absence of vibronic coupling to a vibronic singlet state. The only linear JT systems in which this is known to occur are $H \otimes (g \oplus h)$ [20] and its subsystem $H \otimes h$ [29, 31]. A ground-state crossover is also known to be possible in the quadratic $E \otimes e$ JT system (as can be seen from [32] and [33]) and the $T \otimes t_2$ system [34].

5. The calculation of reduction factors

5.1. First-order RFs

When an electronic perturbation $C_{\Gamma\gamma}$ of symmetry Γ with component γ is present, the corresponding Hamiltonian describing the perturbation within the electronic G states $|G_{\gamma_i}\rangle$ can be written in the form [16]

$$\mathcal{H}^{(1)}(\Gamma) = \sum_{\gamma} W_{\Gamma\gamma} C_{\Gamma\gamma} \tag{25}$$

where the $C_{\Gamma\gamma}$ are orbital operators and the $W_{\Gamma\gamma}$ are corresponding coefficients. The $C_{\Gamma\gamma}$ can be expressed in terms of CG coefficients $\langle \Gamma\gamma g\sigma_j | g\sigma_i \rangle$ by the relation [24]

$$C_{\Gamma\gamma} = \sum_{\sigma_i\sigma_j} |G\sigma_i)(G\sigma_j| \langle \Gamma\gamma G\sigma_j | G\sigma_i \rangle. \tag{26}$$

If the vibronic states derived above are written in the form $|0, G\sigma_i\rangle$, the usual definition of a first-order RF within the ground state is

$$K^{(1)}_{GG}(\Gamma) = \frac{\langle 0, G\sigma_i | C_{\Gamma\gamma} | 0, G\sigma_j \rangle}{(G\sigma_i | C_{\Gamma\gamma} | G\sigma_j)} = \frac{\langle 0, G\sigma_i | C_{\Gamma\gamma} | 0, G\sigma_j \rangle}{\langle \Gamma\gamma G\sigma_j | G\sigma_i \rangle}. \tag{27}$$

The first-order RFs are 'numbers' (dependent upon the coupling strengths and frequencies) which are independent of the components σ_i. As discussed in detail in [16], there are some difficulties in using this definition when repeated representations are involved, as the RF is

then no longer independent of the components used. This must be reflected by expressing the RF in the form of a matrix in the effective Hamiltonian. This will be illustrated in some of the examples given below.

In addition to the RFs acting entirely within a the ground vibronic state, non-zero 'off-diagonal' matrix elements can arise between the ground vibronic state Σ_l and one or more of the tunnelling states Σ_m. Such off-diagonal matrix elements for an operator $C_{\Sigma\sigma_k}$ can be written in the general form

$$K^{(1)}_{\Sigma_l\Sigma_m}(\Sigma) \equiv \frac{\langle 0,\, \Sigma_l\sigma_i|C_{\Sigma\sigma_k}|0,\, \Sigma_m\sigma_j\rangle}{(\Sigma_l\sigma_i|C_{\Sigma\sigma_k}|\Sigma_m\sigma_j)}. \tag{28}$$

5.1.1. First-order reduction factors corresponding to the T wells. On substituting the vibronic states given in equation (9) into the formula for the first-order RF given in equation (27) together with tables 4 and 7 of [24], the relevant RFs are obtained. To illustrate the procedures, we consider the RFs $K^{(1)}_{GG}(T_1)$ and $K^{(1)}_{GG}(T_2)$, choose the orbital operators $\hat{L}_{T_1z}$ and $\hat{L}_{T_2z}$, and use the vibronic states with $\sigma_i \to x$, and $\sigma_j \to y$ given in equation (9), for example. Then

$$\begin{aligned} K^{(1)}_{GG}(T_1) &= \frac{\langle 0G_x|\hat{L}_{T_1z}|0G_y\rangle}{\langle T_1zG_y|G_x\rangle} = -\sqrt{3}\langle 0G_x|\hat{L}_{T_1z}|0G_y\rangle \\ K^{(1)}_{GG}(T_2) &= \frac{\langle 0G_x|\hat{L}_{T_2z}|0G_y\rangle}{\langle T_2zG_y|G_x\rangle} = \sqrt{3}\langle 0G_x|\hat{L}_{T_2z}|0G_y\rangle \end{aligned} \tag{29}$$

with the orbital operators in matrix form given by

$$\hat{L}_{T_1z} = -\frac{1}{\sqrt{3}}\begin{pmatrix} 0 & 0 & 0 & 1 \\ 0 & 0 & 1 & 0 \\ 0 & -1 & 0 & 0 \\ -1 & 0 & 0 & 0 \end{pmatrix}, \qquad \hat{L}_{T_2z} = \frac{1}{\sqrt{3}}\begin{pmatrix} 0 & 0 & 0 & -1 \\ 0 & 0 & 1 & 0 \\ 0 & -1 & 0 & 0 \\ 1 & 0 & 0 & 0 \end{pmatrix}. \tag{30}$$

We then obtain

$$K^{(1)}_{GG}(T_1) = K^{(1)}_{GG}(T_2) = -5(N^T_G)^2 S^T_{12}. \tag{31}$$

In a similar way, the first-order RFs $K^{(1)}_{GG}(H)$ and $K^{(1)}_{GG}(G)$ come from evaluating

$$K^{(1)}_{GG}(H) = \frac{\langle 0G_x|\hat{L}_{H\theta}|0G_x\rangle}{\langle H\theta G_x|G_x\rangle} = -\frac{\sqrt{15}}{2}\langle 0G_x|\hat{L}_{H\theta}|0G_x\rangle \tag{32}$$

with

$$\hat{L}_{H\theta} = -\frac{2}{\sqrt{15}}\begin{pmatrix} 0 & 0 & 0 & 0 \\ 0 & 1 & 0 & 0 \\ 0 & 0 & 1 & 0 \\ 0 & 0 & 0 & -2 \end{pmatrix} \tag{33}$$

We find that the same result is obtained for $K^{(1)}_{GG}(H)$ as was obtained for $K^{(1)}_{GG}(T_1)$ and $K^{(1)}_{GG}(T_2)$. In fact, we can show that the relation

$$K^{(1)}_{GG}(T_1) = K^{(1)}_{GG}(T_2) = K^{(1)}_{GG}(H) \tag{34}$$

must always hold, independent of the model used, using the general theory given in [35] and [36]. This is an example of a RF 'sum rule'. A similar but a slightly more complicated calculation for the remaining first-order RFs gives the result

$$K^{(1)}_{GG}(G) = \tfrac{1}{4}(N^T_G)^2(3 - 8S^T_{12}) \tag{35}$$

with a second sum rule

$$4K^{(1)}_{GG}(G) - K^{(1)}_{GG}(X) = 3 \tag{36}$$

where $X \equiv T_1, T_2$ or H. In the infinite-coupling limit, the overlap $2S_{12}^T$ becomes zero and thus all the above RFs become zero except for $K_{GG}^{(1)}(G)$, which has a limiting value of $\frac{3}{4}$. These limiting values are all in agreement with those found in [14].

Only one non-zero off-diagonal matrix element exists which is given by

$$K_{AG}^{(1)}(G) = \frac{\sqrt{3}}{4}(N_G^T)N_A^T(1 + 4S_{12}^T). \tag{37}$$

5.1.2. First-order reduction factors corresponding to the D_3 wells. The calculation proceeds as for T wells with the relevant symmetry-adapted vibronic ground states given in equation (13). The calculations are straightforward for diagonal operators of T_1, T_2 and G symmetries within the G and H vibronic states and give the result

$$\begin{aligned}
&K_{GG}^{(1)}(T_1) = K_{GG}^{(1)}(T_2) = \tfrac{5}{18}(N_G^{D_3})^2(-3S_{12}^{D_3} + 42S_{13}^{D_3}) \\
&K_{GG}^{(1)}(G) = \tfrac{1}{18}(N_G^{D_3})^2(1 - 12S_{12}^{D_3} + 216S_{13}^{D_3}) \\
&K_{GG}^{(1)}(H) = \tfrac{5}{18}(N_G^{D_3})^2(2 - 6S_{12}^{D_3} + 18S_{13}^{D_3}) \\
&K_{HH}^{(1)}(T_1) = -K_{HH}^{(1)}(T_2) = \frac{5\sqrt{5}}{9\sqrt{2}}(N_H^{D_3})^2\left(-\frac{3}{2}S_{12}^{D_3} - 6S_{13}^{D_3}\right) \\
&K_{HH}^{(1)}(G) = \frac{-\sqrt{5}}{9\sqrt{2}}(N_H^{D_3})^2(1 + 6S_{12}^{D_3} + 18S_{13}^{D_3})
\end{aligned} \tag{38}$$

where the normalizing factors $N_\Gamma^{D_3}$ and overlaps $S_{12}^{D_3}$ and $S_{13}^{D_3}$ are given in section 3.

The case of operators of H symmetry within vibronic states of H symmetry is more complicated. This is because of the repeated representation in the product of $H \otimes H$ (see equation (24)). This problem is very similar to that discussed in Huang *et al* [16] for the $H \otimes (g \oplus h)$ JT system. The first-order RF $K_{HH}^{(1)}(H)$ takes the form of a diagonal 2×2 matrix

$$K_{HH}^{(1)}(H) = \begin{pmatrix} K_{H_a}^{(1)}(H) & 0 \\ 0 & K_{H_b}^{(1)}(H) \end{pmatrix} \tag{39}$$

provided that the labels a and b for the repeated representations are correctly chosen. This occurs when the separation of the CG coefficients follows that of Fowler and Ceulemans [24]. In the present problem we find

$$K_{H_a}^{(1)}(H) = \tfrac{5}{9}(N_H^{D_3})^2(1 + \tfrac{3}{2}S_{12}^{D_3}) \qquad K_{H_b}^{(1)}(H) = 0. \tag{40}$$

The sum rules

$$\begin{aligned}
&4K_{GG}^{(1)}(G) + 5K_{GG}^{(1)}(H) - 6K_{GG}^{(1)}(T_1) = 3 \\
&K_{GG}^{(1)}(T_1) = K_{GG}^{(1)}(T_2)
\end{aligned} \tag{41}$$

relating these RFs are readily obtained. In the case of the D_3 wells, two non-zero off-diagonal matrix elements involving the ground state are present. They are

$$\begin{aligned}
&K_{AG}^{(1)}(G) = \frac{\sqrt{2}}{12}N_G^{D_3}N_A^{D_3}(1 + 3S_{12}^{D_3} + 6S_{13}^{D_3}) \\
&K_{AH}^{(1)}(H) = \tfrac{5}{6}N_G^{D_3}N_A^{D_3}(1 + 3S_{12}^{D_3} + 6S_{13}^{D_3}).
\end{aligned} \tag{42}$$

In figure 5, a selection of the first-order RFs for T wells are plotted as a function of k_g. It is seen that $K_{GG}^{(1)}(T_1)$, $K_{GG}^{(1)}(T_2)$ and $K_{GG}^{(1)}(H)$ start at a value of 1 and decrease exponentially to zero as k_g increases from zero whereas $K_{GG}^{(1)}(G)$ decreases only slightly with k_g and remains finite in strong coupling. Results for D_3 wells are given in figure 6; the RFs also exhibit a

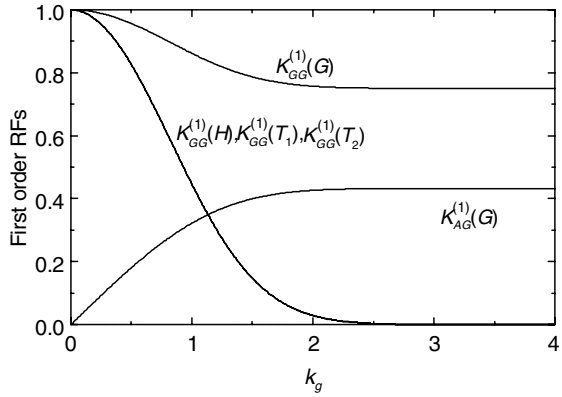

Figure 5. The variation of the first-order RFs as a function of k_g for wells of T symmetry. The $K_{AG}^{(1)}(G)$ off-diagonal RF is also shown.

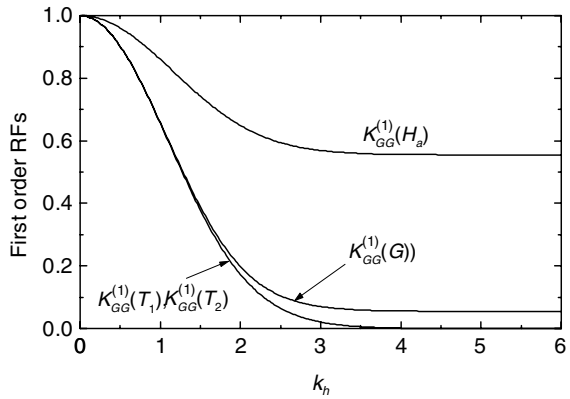

Figure 6. The variation of the first-order RFs as a function of k_h for wells of D_3 symmetry and with $k_g = 0$.

very similar exponential decay to zero as k_g increases but $K_{GG}^{(1)}(G)$ and $K_{GG}^{(1)}(H_a)$ decay to finite values of approximately 0.05 and 0.55 respectively. We note that all off-diagonal RFs are zero for zero vibronic coupling as expected; the example of $K_{AG}^{(1)}(G)$ for T wells is shown in figure 5. Comparison with the results given in [14] is difficult on account of differences in the definitions of the RFs and in their separations when repeated representations are involved.

5.2. Second-order RFs

5.2.1. General principles. The calculation of second-order RFs [13] is much more complicated than that for first-order RFs largely because a summation over an infinite set of excited states is required. Numerical calculations for cubic systems were undertaken by O'Brien [37], for example, and by analytical methods by Bates and Dunn [38,39] and Polinger *et al* [40]. In addition, Liu *et al* [41] have described a general method for the derivation of second-order RFs for the vibronic system based entirely on symmetry grounds. It was later shown that the second-order RFs could be deduced from the evaluation of the sums of various oscillator overlaps [42]. Equivalent calculations in icosahedral symmetry are much

more complicated but nevertheless results have been obtained for the $T_1 \otimes h$ JT system by Qiu *et al* [15] and very recently by Huang *et al* [16] for the $H \otimes (g \oplus h)$ JT system. On account of the complexities involved, simplifications were made in both calculations by taking the excited states to be the harmonic-oscillator states associated with the wells instead of the more accurate symmetry-adapted excited vibronic states such as those derived for the $T_1 \otimes h$ JT system [43]. Although such a simplification is strictly only valid in the infinite-coupling limit, we can nevertheless apply the same procedures and simplifications developed in [16] to the $G \otimes (h \oplus g)$ JT system. Again, for simplicity, we give details only for cases in which the perturbations are the same, although the methods used can readily be extended to all cases. The index labels p and q are needed to distinguish between repeated roots as in the case of the first-order RFs.

On substituting equation (27) into the second-order perturbation Hamiltonian [15, 16]

$$\mathcal{H}^{(2)}(\Gamma \otimes \Gamma) = \mathcal{H}^{(1)}(\Gamma)G(G)\mathcal{H}^{(1)}(\Gamma) \tag{43}$$

where $G(G)$ is the Green operator for the basic electronic G state including summations over all possible phonon excitations and well states, we obtain the general expression

$$K_M^{(2)}(\Gamma \otimes \Gamma) = \frac{\langle 0, G\sigma_i|\mathcal{L}_{M\mu}^{(2)}(\Gamma \otimes \Gamma)|0, G\sigma_j\rangle}{(G\sigma_i|L_{M\mu}^{(2)}(\Gamma \otimes \Gamma)|G\sigma_j)} \tag{44}$$

for the second-order RF in cases in which there are no repeated roots. In equation (44), we define

$$\mathcal{L}_{M\mu}^{(2)}(\Gamma \otimes \Gamma) = \sum_{\gamma_j}\sum_{\gamma_k} C_{\Gamma\gamma_k}^{+} G(G) C_{\Gamma\gamma_j} \langle \Gamma\gamma_j \Gamma\gamma_k | M\mu\rangle \tag{45}$$

and

$$L_{M\mu}^{(2)}(\Gamma \otimes \Gamma) = \sum_{\gamma_j}\sum_{\gamma_k} C_{\Gamma\gamma_k}^{+} C_{\Gamma\gamma_j} \langle \Gamma\gamma_j \Gamma\gamma_k | M\mu\rangle. \tag{46}$$

where $M \in \Gamma \otimes \Gamma$. The second-order contributions to the effective Hamiltonian are then expressed in the form [15]

$$\mathcal{H}_{eff}^{(2)}(\Gamma \otimes \Gamma) = \sum_{M\mu}\sum_{\gamma_j}\sum_{\gamma_k} W_{\Gamma\gamma_k}^{+} W_{\Gamma\gamma_j} \langle \Gamma\gamma_j \Gamma\gamma_k | M\mu\rangle K_M^{(2)}(\Gamma \otimes \Gamma) L_{M\mu}^{(2)}(\Gamma \otimes \Gamma). \tag{47}$$

Each of the repeated representations ($\Gamma = H$ and G) must be treated in a similar way to the first-order RFs by expressing the results in terms of a 2×2 matrix as in Huang *et al* [16].

5.2.2. Evaluation of second-order RFs. Second-order RFs have been calculated for the $G \otimes g$ and $G \otimes h$ subsystems and for the $G \otimes (g \oplus h)$ system separately. We consider each system in turn beginning with the simplest $G \otimes g$ subsystem which involves wells of T symmetry. Detailed calculations show that the corresponding second-order RFs can be written in the form

$$K_M^{(2)}(\Gamma \otimes \Gamma) = -\frac{5}{\hbar\omega_g}\frac{(S_{12}^T)^2}{(4 + S_{12}^T)} G_M(\Gamma) \tag{48}$$

where the functions $G_M(\Gamma)$ are given in table 1. They are expressed in terms of the functions $f_m^T = f(mX_T)$ with $m = \{1, 2\}$ and $X_T = \frac{15}{16}k_g^2$. The function f is defined by [15, 16]

$$f(Z) = \sum_{n=1}^{\infty} \frac{Z^n}{(E + n)n!}. \tag{49}$$

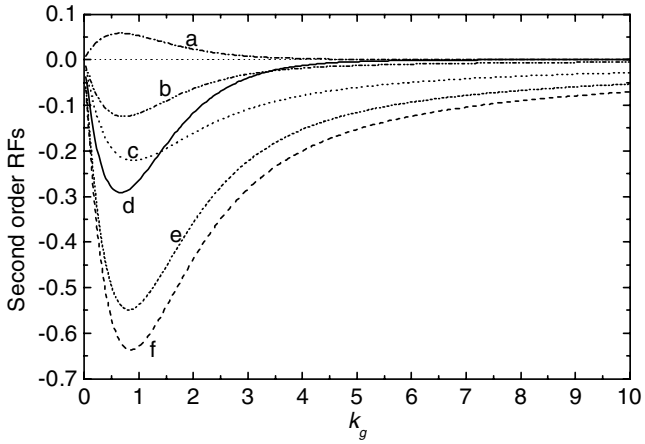

Figure 7. Variation with k_g of the second-order RFs for the $G \otimes g$ JT subsystem. The labelling is defined in the text.

$(E + n)$ corresponds to the difference in energy between an excited vibrational phonon state containing n phonons and the ground vibrational state in units of $\hbar\omega_g$. E is thus given by

$$E = \frac{S_{12}^T}{1 - S_{12}^T} X_T. \tag{50}$$

The possible values of Γ and M which result in non-zero second-order RFs $K_M^{(2)}(\Gamma \otimes \Gamma)$ are also given in table 1. The dependence of the second-order RFs on k_g are displayed graphically in figure 7, with the curves labelled as follows:

a $= K_{T_1}^{(2)}(G \otimes G)$, $K_{T_2}^{(2)}(G \otimes G)$, $K_{H_a}^{(2)}(G \otimes G)$

b $= K_{G_a}^{(2)}(G \otimes G)$

c $= K_A^{(2)}(G \otimes G)$

d $= K_{T_1}^{(2)}(T_1 \otimes T_1)$, $K_{T_1}^{(2)}(T_2 \otimes T_2)$, $K_{T_1}^{(2)}(H \otimes H)$, $K_{T_2}^{(2)}(H \otimes H)$, $K_{H_a}^{(2)}(H \otimes H)$

e $= K_{G_a}^{(2)}(H \otimes H)$

f $= K_A^{(2)}(T_1 \otimes T_1)$, $K_A^{(2)}(T_2 \otimes T_2)$, $K_A^{(2)}(H \otimes H)$.

It is seen that the RFs labelled 'a' are small and positive for all values of k_g whereas the other RFs are always negative and have larger magnitudes.

The second-order RFs for the $G \otimes h$ JT subsystem which involves wells of D_{3d} symmetry wells have also been calculated. The allowed values of Γ and M which result in non-zero second-order RFs $K_M^{(2)}(\Gamma \otimes \Gamma)$ are given in table 2 in terms of the functions $f_m^{D_3} = f(mX_{D_3})$ with $X_{D_3} = \frac{10}{27}k_h^2$. f is the function defined in equation (49), where here we have

$$E = \frac{2(4+T)T}{(6+8T+T^2)} X_{D_{3d}}. \tag{51}$$

The required second order RFs are thus given by

$$K_M^{(2)}(\Gamma \otimes \Gamma) = -\frac{1}{108\hbar\omega_h} \frac{T^2}{(1 + \frac{4}{3}T + \frac{1}{6}T^2)} G_M(\Gamma). \tag{52}$$

Table 1. The functions $G_M(\Gamma)$ used to define the second-order RFs for the $G \otimes g$ JT subsystem involving T wells.

Γ	M	$G_M(\Gamma)$
T_1, T_2	A	$f_1^T + 4f_2^T$
	T_1	$5f_1^T$
G	A	$\frac{1}{5}(-f_1^T + 8f_2^T)$
	T_1, T_2	$-f_1^T$
	G_a	$\frac{1}{10}(14f_1^T + 3f_2^T)$
	H_a	$-f_1^T$
H	A	$f_1^T + 4f_2^T$
	T_1, T_2	$5f_1^T$
	G_a	$2f_1^T + 3f_2^T$
	H_a	$5f_1^T$

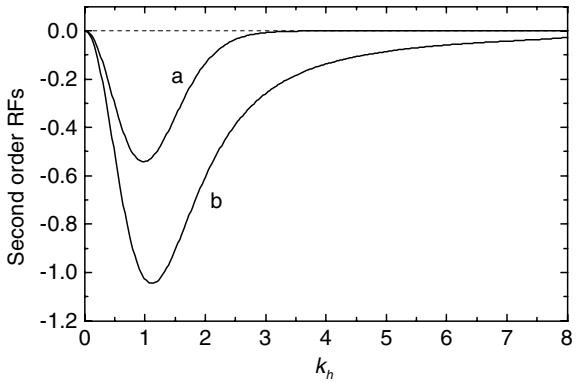

Figure 8. Plots of some second-order RFs from the $G \otimes h$ JT subsystem.

The functions $G_M(\Gamma)$ can be obtained directly from table 2. A selection of the RFs are displayed in figure 8, labelled a and b where

$$\text{a} = K_{T_1}^{(2)}(T_1 \otimes T_1),\ K_{T_2}^{(2)}(T_2 \otimes T_2),\ K_H^{(2)}(T_1 \otimes T_1),\ K_H^{(2)}(T_2 \otimes T_2)$$
$$\text{b} = K_A^{(2)}(T_1 \otimes T_1),\ K_A^{(2)}(T_2 \otimes T_2)$$

Finally, we determine second-order RFs for the $G \otimes (g \oplus h)$ JT system for D_3 wells. These are given by

$$K_M^{(2)}(\Gamma \otimes \Gamma) = -\frac{1}{108\hbar\omega_h}\frac{t^2}{T^4}\frac{1}{\sqrt{1 + 2S_{12}^{D_3} + S_{13}^{D_3}}}G_M(\Gamma). \tag{53}$$

The functions $G_M(\Gamma)$ and the possible values of M and Γ which give non-zero values for $K_M^{(2)}(\Gamma \otimes \Gamma)$ are given in table 3. The results are expressed in terms of the quantities F_i where

Table 2. The functions $G_M(\Gamma)$ used to define the second-order RFs for the $G \otimes h$ JT subsystem involving D_{3d} wells.

Γ	M	$G_M(\Gamma)$
T_1, T_2	A	$5(40f_3^{D_3} + 3f_2^{D_3} + 42f_4^{D_3})s^2 + 40(4f_2^{D_3} + f_1^{D_3})s + 60f_2^{D_3}$
	T_1, T_2	$100(3f_2^{D_3} + f_3^{D_3})s^2 + 50(4f_1^{D_3} + f_2^{D_3})s$
	H	$100(3f_2^{D_3} + f_3^{D_3})s^2 + 50(4f_1^{D_3} + f_2^{D_3})s$
G	A	$(23f_2^{D_3} + 232f_3^{D_3} + 216f_4^{D_3})s^2 + 8(3f_1^{D_3} + 14f_2^{D_3})s + 48f_2^{D_3}$
	T_1	$15(29f_2^{D_3} + 2f_3^{D_3})s^2 + 80(f_1^{D_3} + f_2^{D_3})s$
	T_2	$15(29f_2^{D_3} + 2f_3^{D_3})s^2 + 80(f_1^{D_3} + f_2^{D_3})s$
	G_a	$(319f_2^{D_3} + 76f_3^{D_3} + \frac{41}{2}f_4^{D_3})s^2 + 8(19f_1^{D_3} + 7f_2^{D_3})s - 6f_2^{D_3}$
	H_a	$5(-f_2^{D_3} + 44f_3^{D_3} + 32f_4^{D_3})s^2 + 40(5f_1^{D_3} + 2f_2^{D_3})s$
H	A	$5(f_2^{D_3} + 8f_3^{D_3} + 18f_4^{D_3})s^2 + 160f_2^{D_3}s + 120f_2^{D_3}$
	T_1, T_2	$50(4f_1^{D_3} + f_2^{D_3})s$
	G_a	$5(-4f_4^{D_3} + 17f_2^{D_3} - 4f_3^{D_3})s^2 + 20(10f_1^{D_3} + f_2^{D_3})s + 15f_2^{D_3}$
	H_a	$\frac{25}{2}(5f_2^{D_3} + 2f_3^{D_3} + 2f_4^{D_3})s^2 + 25(2f_1^{D_3} + 5f_2^{D_3})s + 75f_2^{D_3}$

Table 3. The functions $G_M(\Gamma)$ used to define the second-order RFs for the $G \otimes (h \oplus g)$ JT system involving D_3 wells.

Γ	M	$G_M(\Gamma)$
T_1, T_2	A	$10(-F_5 + 6F_2)S^2T^2 + 40(F_1 + 4F_6)ST + 5(40F_3 + 42F_4 + 3F_6)$
	T_1, T_2, H	$25S^2T^2F_5 + 50(F_6 + 4F_1)ST + 100(3F_6 + F_3)$
G	A	$4(-F_5 + 12F_2)S^2T^2 + 8(3F_1 + 14F_6)ST + (232F_3 + 216F_4 + 23F_6)$
	T_1, T_2	$20S^2F_5T^8 + 80(F_6 + F_1)ST + 5(87F_6 + 6F_3)$
	G_a	$2(14F_5 - 3F_2)S^2T^2 + 8(19F_1 + 7F_6)ST + (76F_3 + \frac{41}{2}F_4 + 319F_6)$
	H_a	$-20T^8S^2F_5 + 40(5F_1 + 2F_6)ST + 5(44F_3 + 80F_4 - F_6)$
H	A	$20(6F_2 + F_5)S^2T^2 + 160F_6ST + 5(8F_3 + 18F_4 + F_6)$
	T_1, T_2	$125S^2T^2F_5 + 50(4F_1 + F_6)ST$
	G_a, G_b	$5(3F_2 + 23F_5)S^2T^2 + 20(10F_1 + F_6)ST + 5(17F_6 - 4F_3 - 4F_4)$
	H_a, H_b	$\frac{25}{2}(6F_2 + 5F_5)S^2T^2 + 25(2F_1 + 5F_6)ST + \frac{25}{2}(2F_3 + 2F_4 + 5F_6)$

$F_i = f(y_i)$ with

$$\begin{aligned} y_1 &= \tfrac{5}{54}k_g^2 + \tfrac{10}{27}k_h^2 \\ y_2 &= \tfrac{5}{27}k_g^2 + \tfrac{20}{27}k_h^2 \\ y_3 &= \tfrac{10}{9}k_h^2 \\ y_4 &= \tfrac{5}{54}k_g^2 + \tfrac{40}{27}k_h^2 \\ y_5 &= \tfrac{5}{36}k_g^2 \\ y_6 &= \tfrac{5}{108}k_g^2 + \tfrac{20}{27}k_h^2. \end{aligned} \tag{54}$$

The energy difference is given by

$$E = -\frac{5}{108}\frac{(-4S_{12}^{D_3} + S_{13}^{D_3})k_g^2 - 16(S_{12}^{D_3} - S_{13}^{D_3})k_h^2}{(1 - 2S_{12}^{D_3} + S_{13}^{D_3})}. \tag{55}$$

Some of the second-order RFs are plotted in figure 7. When we set the $k_g = 0$, all the above expression can be simplified to the corresponding second-order RFs of the $G \otimes h$ subsystem.

6. Discussion and conclusions

The $G \otimes (g \oplus h)$ JT system and the associated $G \otimes g$ and $G \otimes h$ JT subsystems have been studied in detail in order to obtain theoretical background information on the vibronically coupled orbital quadruplet in icosahedral symmetry. Previously published work on these systems has been severely limited in contrast to that on the $T \otimes h$ and $H \otimes (g \oplus h)$ JT systems. This is because the T and H electronic states form the ground states of the C_{60}^{-} and C_{60}^{+} ions respectively. Nevertheless, the $G-$ orbital state can appear as an excited orbital state of these ions or of neutral C_{60}. Excited states can be very important in some situations in which the identification and modelling of experimental data is required. This can properly only be done if the properties of the system have been clearly established, and this has been the aim of this paper.

One of the most productive mechanisms for interpreting experimental data involving G states is likely to involve using an appropriate effective Hamiltonian in which perturbations are expressed in terms of orbital and spin operators only, whilst the effects of the phonon spectrum and their interactions appear as parameters in the form of RFs. Determination of the latter for the G-orbital state has been the prime objective of this paper. Expressions for the first- and second-order RFs for the wells in the $G \otimes (g \oplus h)$ JT system (and corresponding subsystems) have been calculated using symmetry-adapted ground states and excited states located in the T and D_3 minima.

In order to undertake the RF calculations, it was first necessary to find expressions for the vibronic states. This was accomplished by first finding expressions for vibronic states localized in wells in the APES and then introducing tunnelling by constructing linear combinations of the well states, transforming with the appropriate symmetries, using projection operator techniques. This method also ensures that the relative phases associated with each of the well states is automatically correct and the Berry phase need not be explicitly included. The energies corresponding to the resultant symmetry-adapted states were then calculated. As a result, it was found that there is a region of coupling to the g and h modes for which the ground state is a vibronic A state. Although this lies outside the range of validity of our results in linear coupling, it does suggest the possibility that the ground state may actually be a vibronic singlet if significant higher-order couplings are present. However, the inclusion of such terms requires much extra work that is beyond the scope of this paper. Nevertheless, this observation could have far-reaching consequences. Spectroscopic results indicating an A state would not obviously suggest the presence of a $G \otimes (g \oplus h)$ JT effect, even though this could be the case. Furthermore, in the regimes where the A state is lowest, it will not be possible to model the vibronic system by an effective Hamiltonian based on G states, as would otherwise be expected. The situation should be compared to the $H \otimes (g \oplus h)$ and $H \otimes h$ JT systems, for which a ground-state crossover can occur in linear coupling.

The results presented in this paper should provide much of the information required to model real JT systems derived from an electronic G state.

Acknowledgment

MA-G would like to thank the University Research Board of the American University of Beirut for a long-term travel grant.

References

[1] Ceulemans A and Fowler P W 1989 *Phys. Rev.* A **39** 481
[2] Gu B, Li Z and Zhu J 1993 *J. Phys.: Condens. Matter* **5** 5255
[3] Judd B R 1957 *Proc. R. Soc.* A **241** 122
[4] Wiseman R W 1998 *J. Phys. A: Math. Gen.* **31** 7647

[5] Backhouse N B and Gard P 1974 *J. Phys. A: Math. Gen.* **7** 2101
[6] Pooler D R 1980 *J. Phys. C: Solid State Phys.* **13** 1029
[7] Longuet-Higgins H C and Roberts M de V 1955 *Proc. R. Soc.* A **230** 110
[8] Hawthorne M F and Pittochelli 1960 *J. Am. Chem. Soc.* **82** 3228
[9] Greenwood N N and Earnshaw A 1984 *Chemistry of the Elements* (New York: Pergamon)
[10] Khlopin V P, Polinger V Z and Bersuker I B 1978 *Theor. Chim. Acta (Berlin)* **48** 87
[11] Cullerne J P and O'Brien M C M 1994 *J. Phys.: Condens. Matter* **6** 9017
[12] Chancey C C and O'Brien M C M 1997 *The JT Effect in C_{60} and other Icosahedral Complexes* (Princeton, NJ: Princeton University Press)
[13] Ham F S 1965 *Phys. Rev.* A **138** 1727
[14] Cullerne J P, Angelova M N and O'Brien M C M 1995 *J. Phys.: Condens. Matter* **7** 3247
[15] Qiu Q C, Dunn J L, Bates C A, Abou-Ghantous M and Polinger V Z 2000 *Phys. Rev.* B **62** 16 155
[16] Huang R, Abou-Ghantous M, Bates C A, Dunn J L, Polinger V Z and Moate C P 2002 *J. Phys.: Condens. Matter* **14** 1319
[17] Bates C A, Dunn J L and Sigmund E 1987 *J. Phys. C: Solid State Phys.* **20** 1965
Bates C A, Dunn J L and Sigmund E 1987 *J. Phys. C: Solid State Phys.* **20** 4015 (corrigendum)
[18] Öpik U and Pryce M H L 1957 *Proc. R. Soc.* A **238** 425
[19] Dunn J L and Bates C A 1995 *Phys. Rev.* B **52** 5996
[20] Moate C P, Dunn J L, Bates C A and Liu Y M 1997 *J. Phys.: Condens. Matter* **9** 6049
[21] Rough S M, Dunn J L and Bates C A 1997 *Z. Phys. Chem.* **200** 129
[22] O'Brien M C M 1972 *J. Phys. C: Solid State Phys.* **5** 2045
[23] Boyle L L and Parker Y V 1980 *Mol. Phys.* **39** 95
[24] Fowler P W and Ceulemans A 1985 *Mol. Phys.* **54** 767
[25] Ceulemans A 1987 *J. Chem. Phys.* **87** 5374
[26] O'Brien M C M 1969 *Phys. Rev.* **187** 407
[27] Judd B R 1974 *Can. J. Phys.* **52** 999
[28] Hallam L D, Bates C A and Dunn J L 1992 *J. Phys.: Condens. Matter* **4** 6775
[29] Moate C P, O'Brien M C M, Dunn J L, Bates C A, Liu Y M and Polinger V Z 1996 *Phys. Rev. Lett.* **77** 4362
[30] Liu Y M, Dunn J L and Bates C A 1994 *J. Phys.: Condens. Matter* **6** 7521
[31] De Los Rios P, Manini N and Tosatti E 1996 *Phys. Rev.* **54** 7157
[32] Zwanziger J W and Grant E R 1987 *J. Chem. Phys.* **87** 2954
[33] Ham F S 1987 *Phys. Rev. Lett.* **58** 725
[34] Koizumi H, Bersuker I B, Boggs J E and Polinger V Z 2000 *J. Chem. Phys.* **112** 8470
[35] Payne S H and Stedman G E 1983 *J. Phys. C: Solid State Phys.* **16** 2679
[36] Oliete P B, Bates C A and Dunn J L 1999 *Phys. Rev.* **60** 2319
[37] O'Brien M C M 1990 *J. Phys.: Condens. Matter* **2** 5539
[38] Bates C A and Dunn J L 1989 *J. Phys.: Condens. Matter* **1** 2605
[39] Dunn J L and Bates C A 1989 *J. Phys.: Condens. Matter* **1** 2617
[40] Polinger V Z, Bates C A and Dunn J L 1991 *J. Phys.: Condens. Matter* **3** 513
[41] Liu Y M, Dunn J L and Bates C A 1994 *J. Phys.: Condens. Matter* **6** 859
[42] Liu Y M, Dunn J L and Bates C A 1997 *J. Phys.: Condens. Matter* **9** 7119
[43] Qiu Q C, Dunn J L and Bates C A 2001 *Phys. Rev.* B **64** 075102